KURING Wind Tunnel: Aerodynamic Characteristics Tests of Road Vehicles in Time-Dependent Winds

MASARU SUMIDA
Department of Mechanical Engineering, Faculty of Engineering
Kindai University
1 Takaya Umenobe, Higashi-Hiroshima
JAPAN
sumida@hiro.kindai.ac.jp http://www.hiro.kindai.ac.jp/en/faculty/mechanical/index.html

Abstract: An advanced wind tunnel has been introduced as a facility for road vehicle development at the Kindai University (KURING). In this paper, the features of this wind tunnel, which can generate arbitrary patterns of time-varying wind velocities, are first described. There are four representative airflow patterns: steady wind with constant velocity, pulsating wind with oscillating velocity, gusts of wind, and stepwise-varying wind. The patterns are programmable and easy to operate. Using this wind tunnel, a basic test under unsteady wind conditions was conducted to obtain the characteristics of the fluid forces on the vehicle model subjected to the pulsating wind. Then, the different influences of the wind oscillation on the fluid forces acting on the model were discussed. It was concluded that wind oscillation produces striking effects on the vehicles. These results suggest that it is very important to test vehicles under unsteady wind conditions, and that this wind tunnel is very useful to investigate the unsteady aerodynamics of road vehicles.

Key-Words: Advanced Wind Tunnel, Road Vehicle, Time-Dependent Wind, Fluid Force, Ahmed Model, Pulsating Wind

1 Introduction

In the automotive industry, besides improving the safe performance of road vehicles, the requirements for reducing drag forces are now greater [1]. Consequently, in manufacturing facilities, practical tests of road vehicles are carried out. Looking at recently built wind tunnels, they are becoming larger and have changed in type, from fixed to movable floor wind tunnels. However, in these wind-tunnel experiments [2], the aerodynamic characteristics of vehicles are only examined at a constant wind speed. The vehicles ordinarily encounter air with atmospheric fluctuations. Therefore, it is desirable to study the characteristics of the aerodynamic forces acting on vehicles not only under the conventional conditions of steady wind but also under unsteady wind [3–5].

In response to these requirements, Kindai University started research on car technologies through the cooperation of industry and university [6]. For this research, an advanced wind tunnel was set up at the Kindai University Research Institute of Fundamental Technology for Next Generation (KURING). By using this wind tunnel, we can systematically investigate the unsteady aerodynamic characteristics of road vehicles under variable wind conditions. This wind tunnel is able to generate, in a programmable way, time-dependent airflows such as pulsating, gust, and stepwise-varying winds.

Greenblatt [7] has described a method for obtaining large-scale variations in airflow speeds in wind tunnels. Moreover, he has analyzed a particular method based on louvers with multiple variable vanes. In regards to wind tunnels in Japan generating time-dependent airflows, Yagi [8] reported on their methods and equipment.

In this paper, we first present a summary of the characteristics of the wind tunnel set up in KURING. Second, we describe a basic experiment conducted at the beginning of the research on the aerodynamic characteristics of road vehicles subjected to unsteady airflow. Finally, we present the obtained results for pulsating airflow.

2 Test System of Advanced Wind-Tunnel

2.1 Outlook of Wind Tunnel

The appearance and dimensions of the advanced wind tunnel in KURING are shown in Figs. 1 and 2, respectively. The wind tunnel has a nozzle, whose exit is a square cross section with a 600 mm side. Depending on the experiment, three types of air

Fig. 1 Overall view of wind tunnel

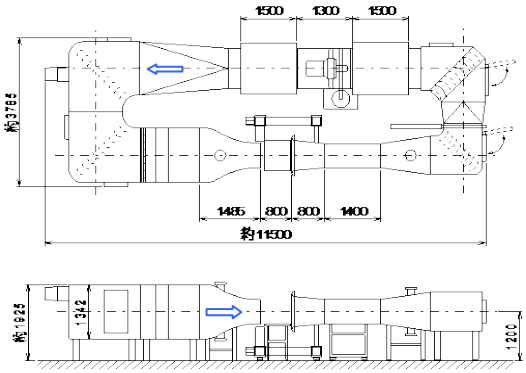

Fig. 2 Schematic diagram of wind tunnel

Fig. 3 Photograph of operating panel

circuits can be made by setting up and/or combining the air trunks: closed return type; semi-open return type; and open, no return type. Thus, it is possible for us to use this facility for various studies.

A great advantage of this facility is that it is equipped with an axial flow blower with both a rotor blade pitch-changeable control and a rotational speed control. The axial flow blower is driven with a 200 V and 45 kW electric motor. The rated flow,

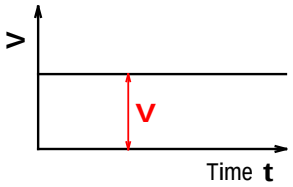

(a) Steady wind mode

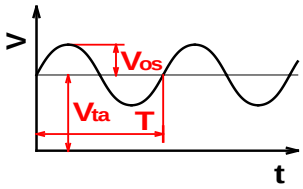

(b) Pulsating wind mode

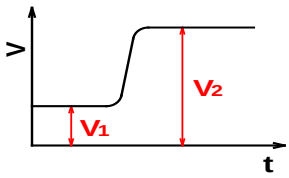

(c) Gust mode

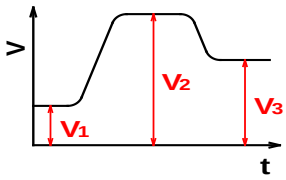

(d) Stepwise-varying wind mode

Fig.4 Wind modes

speed, and static pressure of the axial flow blower are 900 m^3/min, 1755 rpm, and 785 Pa, respectively. Wind speed, which may change in various patterns, can be programmed and repeatedly generated by 1) properly adjusting the minimum and maximum pitch-angles of the rotor blades; 2) introducing the interval time of the pitching motion. For steady wind, the available speed ranges from 1.5 to 45 m/s.

The contraction section is 1.485 m in length, with a rate of contraction of approximately 5:1. The ground plane is equipped with a 300 mm diameter turntable, in order to change the angle of the wind direction against the car model.

2.2 Mode of Wind Velocity

Figure 3 shows the photograph of the panel to operate the wind tunnel. The operating system consists of flow velocity sensors, controls to drive the electric motor and axial flow blower, and a boundary-layer control. These components are

operated and are monitored with the personal computer.

The velocity of the airflow issued from the wind tunnel nozzle is measured with both the Pitot tube and hot-wire anemometry. In this wind tunnel, we can drive various modes of wind speed. The wind modes are of four main types, steady wind, pulsating wind, gust, and stepwise-varying wind modes, as shown in Fig. 4. For the pulsating-wind mode in Fig. 4(b), there are different procedures for rotor blade control and for rotational speed control. In the fourth mode in Fig. 4(d), we can change the wind speed in steps, V_1 to V_{20}.

3 Experimental Apparatus and Measurement Procedures for the Basic Experiment

Figure 5 shows the schematic diagram of the basic experiment carried out with the semi-open-type wind tunnel. The drag, side, and lift forces (*D*, *S*, and *L*, respectively) applied to the vehicle model are detected by the multi-component load cell (Nissho-Electric-Works Co., LMC 3502). The output voltages of the load cell are amplified with direct current amplifiers. They are converted to digital quantities through a data collection system and are then processed in the personal computer. The static pressures on the vehicle model are measured using diffusive-type semiconductor differential pressure transducers (JTEKT Co., DD101K) together with digital pressure gauges (OKANO WORKS Ltd., DMC). Additionally, their output voltages are processed with the above-mentioned data collection system.

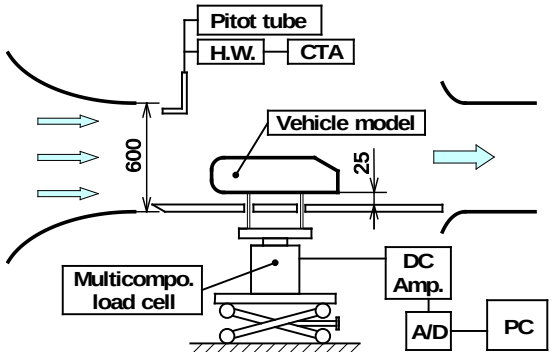

Fig. 5 Schematic diagram of experimental apparatus

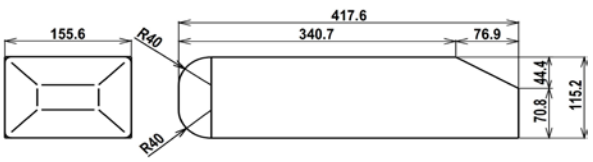

Fig. 6 Road vehicle model (Ahmed-type model [9] with a slant angle of 30°)

Figure 6 shows the vehicle model employed in the present basic experiments. We use the Ahmed-type model [9] with a slant angle of 30°, because until now, most data had been accumulated in steady airflow. The size of the model is such that the blockage ratio of the wind tunnel does not exceed 1/20. Thus, the test model is approximately 1/12.5 of a practical vehicle. The model is supported by four columns 6 mm in diameter.

4 Results and Discussion

In this report, we deal with the problem that the relative velocity of the vehicle against the wind is only in the flow direction when the vehicle is going straight. Furthermore, we consider the case when road vehicles receive pulsating wind. Then, we discuss the influences of the oscillating wind on the fluid forces. Figure 7 shows an example of the obtained results. The experiments were conducted under pulsating wind conditions, i.e., the wind changes with a pulsation period of $T = 1.5$ s. In Fig. 7, the vertical axis shows the drag and lift forces, *D* and *L*, and the wind velocity *V*. The wind velocity changes almost sinusoidal with time *t* and can be simply expressed by the following equation:

$$V(t) = V_{ta} + V_{os} \bullet \sin\Theta, \qquad (1)$$

where Θ (= ωt) is the phase angle, and ω being the pulsation frequency. The subscripts of *ta* and *os*

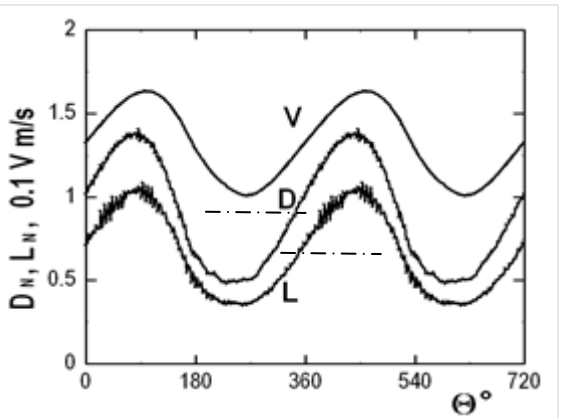

Fig. 7 Changes in drag and lift forces with time under pulsating wind condition

indicate time-mean and amplitude values, respectively. According to this expression, the time-mean and oscillating components of the wind in Fig. 7 are V_{ta} = 13.2 m/s and V_{os} = 3.1 m/s, respectively. They give the amplitude ratio of η = 0.235. The dashed and dotted lines in the figure show the time-mean values.

The time-mean drag and lift forces, D_{ta} and L_{ta}, is approximately 10% larger than the drag and lift forces under steady wind, with the same value as the time-averaged velocity of the pulsating wind. Moreover, the oscillating components, D_{os} and L_{os}, are equivalent to approximately 50% of the time-mean values, D_{ta} and L_{ta}, though the oscillating ratio η is approximately 0.24. In addition, there occurs the phase difference in oscillation between the wind and the fluid forces. That is, the drag and lift forces vary with the phase leads of 15° and 10°, respectively, from the oscillation of the wind. Therefore, it is understood that the oscillation of the wind speed has a striking effect on the vehicles.

Next, the relations between the fluid forces and the wind velocity for a cycle are shown in the form of a Lissajous diagram in Fig. 8. In the figure, the drag and lift forces, D and L, are normalized by the dynamic pressure, $\rho V_{ta}^2/2$, with the time-mean velocity, V_{ta}, of the wind, i.e.,

$$\left.\begin{aligned} C_D(t) &= D/(A\rho V_{ta}^2/2), \\ C_L(t) &= L/(A\rho V_{ta}^2/2). \end{aligned}\right\} \qquad (2)$$

Here, ρ is the air density, and A is the projected frontal area of the vehicle model. In the figures, the horizontal axis is the non-dimensionalized oscillating velocity of the wind, $(V-V_{ta})/V_{os}$. The horizontal arrows indicate the time-mean value.

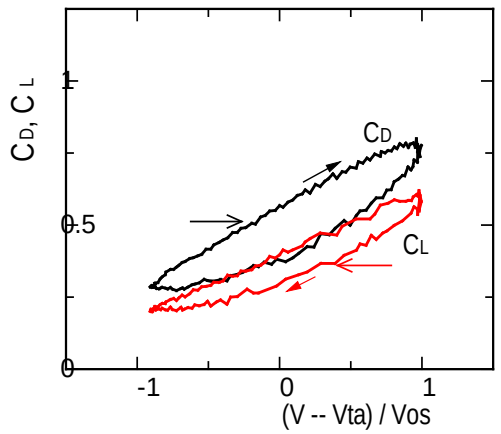

Fig. 8 Lissajous diagram of drag and lift coefficients

The C_D and C_L change in a clockwise direction with time. As seen from Fig. 8, the drag force approximately increases in proportion to the wind speed, when the head wind becomes strong. On the contrary, it decreases rapidly for the first half of the phase when the wind weakens. The reason could be as follows. For vehicles with a slant angle of 30°, there occurs a reduction in pressure in the upper part of the rear of the bodies due to a large-scale vortex, which is well known from the work of Ahmed et al. [9]. The pressure reduction causes C_D and C_L to increase. Accordingly, the C_D and C_L change in the strength of the vortex motion, which is dependent on the acceleration and deceleration of the wind speed. The difference in the drag force between an increasing and a decreasing flow-speed is larger than that in the lift force

5 Concluding Remarks

In this paper, we reported on the testing of road vehicles using the wind tunnel set up in KURING, with the purpose of contributing to the technical development of road vehicles. The conventional wind tunnel and its test technologies have been developed for steady wind conditions. As seen from the results obtained under pulsating wind conditions, the influence of the wind-speed oscillation on aerodynamic characteristics is significant. Nevertheless, the evaluation of the aerodynamic characteristics under unsteady flow conditions, assuming a natural environment, is not easy to perform with the real car wind tunnel because of the cost of the equipment. Although our wind tunnel is not too large, airflow modes that correspond to these problems can be programmed and reproduced. Thus, our wind tunnel is expected to be highly useful for the research of fluid-force characteristics of vehicles under unsteady wind conditions, which are not yet known.

Acknowledgements:

The author would like to thank Mr. S. Morita for his assistance with the experiments during his time as a graduate student. This work was supported by MEXT-Supported Program for the strategic research foundation at private universities (Grant No. S0901045), whose representative was Prof. H. Kyogoku [6], and also in part by the Japan Climate Systems Corporation.

References:

[1] Kaneko, M., Wind Tunnel Technologies for Automobile Development, *Wind Tunnel Symposium 2015*, Atsugi, 2015.

[2] Takagi, M., Automotive Wind Tunnels, *Journal of the Visualization Society of Japan*, Vol. 32, No. 124, 2012, pp. 9-13.

[3] Wordley, S. and Saunders, J., On-road turbulence, *SAE Paper*, No. 2008-01-0475, 2008.

[4] Fuller, J., Best, M., Garret, N. and Passmore, M., The Importance of Unsteady Aerodynamics to Road Vehicle Dynamics, *Journal of Wind Engineering and Industrial Aerodynamics*, Vol. 117, 2013, pp. 1-10.

[5] Liu, X., Han, Y., Cai, C. S., Levitan, M. and Nikitopoulos, D., Wind Tunnel Tests for Mean Wind Loads on Road Vehicles, *Journal of Wind Engineering and Industrial Aerodynamics*, Vol. 150, 2016, pp. 15-21.

[6] Kyogoku, H. ed., *Report of Study on Development of Automobile Technologies in Cooperation with University and the Industry [MEXT-Supported Program (Grant No. S0901045)], 1st Report: FY 2009 to 2010*, Research Institute of Fundamental Technology for Next Generation, Kindai University, 2011.

[7] Greenblatt, D., Unsteady Low-Speed Wind Tunnels, *AIAA Journal*, Vol. 54, No. 6, 2016, pp. 1817-1830.

[8] Yagi, T., Generation of Unsteady Flows in the Wind Tunnel, *Wind Engineers. Japan Association for Wind Engineering*, Vol. 34, No. 1, 2009, pp. 30-35.

[9] Ahmed, S. R. and Ramm, G., Some Salient Features of the Time-Averaged Ground Vehicle Wake, *SAE Paper*, No. 840300, 1984.